The Hilbert-Huang Transform in Engineering

Edited by

Norden Huang
Nii O. Attoh-Okine

Taylor & Francis
Taylor & Francis Group

Boca Raton London New York Singapore

A CRC title, part of the Taylor & Francis imprint, a member of the Taylor & Francis Group, the academic division of T&F Informa plc.

2005

4 A Comparison of the Energy Flux Computation of Shoaling Waves Using Hilbert and Wavelet Spectral Analysis Techniques

Paul A. Hwang, David W. Wang, and James M. Kaihatu

CONTENTS

ABSTRACT

The HHT analysis interprets wave nonlinearity in terms of frequency modulation instead of harmonic generation. The resulting spectrum energy concentrates in the neighborhood of the fundamental frequency in comparison with the FFT or wavelet spectrum. The energy flux computation from the HHT spectrum is considerably larger than with the FFT or wavelet spectrum.

4.1 INTRODUCTION

Fourier transform decomposes a nonlinear waveform into a fundamental frequency component and its harmonics. As a result, the energy of a nonlinear wave is spread into higher frequencies. This may produce difficulties in the interpretation of wave propagation and quantification of wave dynamic properties such as the energy flux of the wave field. Recently, Norden Huang and his colleagues developed a new analysis technique, the Hilbert-Huang transformation (HHT). Through analytical examples, they demonstrated the excellent frequency and temporal resolution of HHT for analyzing nonstationary and nonlinear signals [1, 2].

With the HHT analysis, the physical interpretation of nonlinearity is frequency modulation, which is fundamentally different from harmonic generation. The HHT spectrum therefore retains its energy density near the fundamental frequency of the wave motion in comparison with the FFT or wavelet spectrum [3]. In this article, we briefly describe the HHT technique and investigate its use in the calculation of the energy flux of ocean waves. The resulting HHT spectrum is compared with the counterpart obtained by the wavelet method. The wavelet technique is based on Fourier spectral analysis but uses adjustable frequency-dependent window functions — the mother wavelets — to provide temporal/spatial resolution for nonstationary signals [4–7]. As expected, the Fourier-based analysis interprets wave nonlinearity in terms of harmonic generation; thus the spectral energy leaks to higher frequency components. The HHT interprets wave nonlinearity as frequency modulation, and the spectral energy remains near the base frequency. The computed energy flux from the HHT method is much higher than that from the wavelet method.

4.2 THE HUANG-HILBERT SPECTRAL ANALYSIS

Hilbert transformation was introduced to water wave analysis in the 1980s. Applications include the study of wave modulation leading to wave breaking [8], local properties of sea waves such as the group and pulse structure, fluctuation of wave energy and energy flux [9], and the measurement and quantification of breaking events of wind-generated surface waves [10]. A key function of the Hilbert analysis is the derivation of local wave number in a spatial series or instantaneous frequency in a time series. To use the Hilbert transformation, proper preprocessing of the signals is critical. Large errors in the computed local frequency or wave number can occur when small waves are riding on longer waves or when sharp changes of the oscillation frequencies occur in the wave signal. Quantitative discussions on the riding

wave problem [1] and on the rapid change of the oscillation frequencies [11] have been published and will not be repeated here.

The key ingredient in the HHT is empirical mode decomposition (EMD), designed to reposition the riding waves at the mean water level. This is achieved through a sifting process that repeatedly subtracts the local mean from the original signals. The procedure decomposes the signal into many modes with different frequency characteristics, and thus also alleviates the problem of sharp frequency change in the original signal. Huang and his coworkers have provided extensive discussions on the EMD [1, 2]. From experience, even for very complicated random signals, a time series can usually be decomposed into a relatively small number of modes, $M < \log_2 N$. Each mode is free of riding waves and is suitable for Hilbert transformation to yield accurate local frequency of the mode. The spectrum of the original signal can be obtained from the sum of the Hilbert spectra of all modes. Extensive tests have been carried out, and the HHT technique proves to deliver very high frequency and temporal/spatial resolutions in analyzing nonstationary signals. It is also shown to be able to handle the task of analyzing nonlinear signals produced by exact solution with modulating oscillation frequencies, whereas Fourier-based techniques interpret the signals as superposition of harmonics [1–3].

4.3 SHOALING WAVES AND ENERGY FLUX COMPUTATION

The Hilbert view of nonlinear waves is significantly different from the conventional Fourier view. In particular, intra-wave modulation is a key signature of nonlinearity based on the Hilbert spectral analysis, while harmonic generation is typical of the Fourier spectrum. The difference in the interpretations of nonlinearity will lead to quantitative differences in the energy flux computation.

4.3.1 FIELD MEASUREMENT

An example of intra-wave modulation highlighted by the HHT analysis is illustrated in the analysis of shoaling swell shown in Figure 4.1. The three-dimensional (3D) surface wave topography was acquired by an airborne topographic mapper (ATM, an airborne scanning laser system) near Duck, N.C., three days after an extratropical storm passed through the area. The wind condition at the time of data acquisition was low, resulting in a relatively simple two-dimensional (2D) swell system propagating on mild slope bathymetry. More discussions of the environmental conditions, measurement techniques, and the bathymetry of the region are reported by Hwang et al. [12]. Figure 4.1 illustrates the spatial evolution of the airborne measured shoaling swell (Plot a), the Hilbert spectrum (Plot b), and the wavelet spectrum (Plot c) in the near coast region. For reference, the water depth based on the bathymetry database is shown in Plot d. The spectral energy is distributed narrowly about the dominant frequency. The distinctive intra-wave modulation in the neighborhood of the peak frequency of the wave spectrum can be clearly identified in the HHT spectrum (Figure 4.1b). In contrast, the wavelet spectrum distributes the energy into harmonics, as a result of interpreting nonlinearity as harmonic generation in the

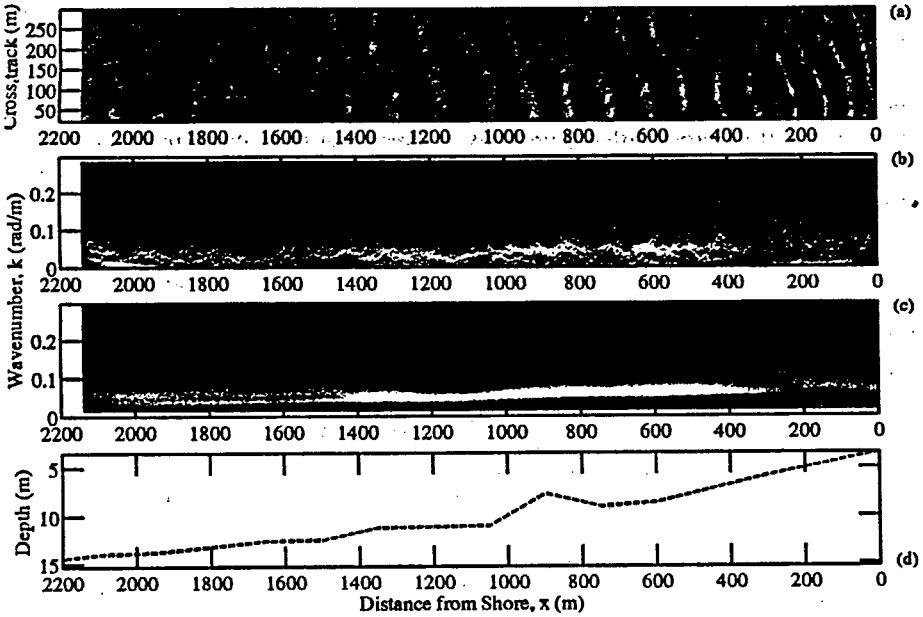

FIGURE 4.1 (*a*) A 3D surface wave topography of shoaling swell in the coastal region. (*b*) The HHT spectrum of the waves shown in (*a*). (*c*) The wavelet spectrum of the waves shown in (*a*). (*d*) The water depth from bathymetry database.

Fourier-based spectral processing (Figure 4.1c), as discussed earlier. It is noticeable that the second harmonic of the wavelet spectrum displays a spatial modulation characteristic similar to the intra-wave modulation of the HHT spectrum at the peak frequency.

The energy flux, F, of the wave field can be computed from the wave spectrum, S, by

$$F(x) = \int S(\omega;x) C_g(\omega;x) d\omega \,, \tag{4.1}$$

where x is the spatial coordinate in the propagation direction, ω is angular frequency, and C_g is the wave group velocity. The computed results based on HHT and wavelet analyses are shown in Figure 4.2. The magnitude derived from the Hilbert spectrum is in general larger than that obtained by the wavelet spectrum. As explained in the last section, this is partly caused by the much higher spectral level in the lower frequency of the Hilbert spectrum compared to the wavelet spectrum. Because phase velocity and group velocity of gravity waves increase monotonically with wavelength, the increased low frequency spectral density translates to a higher level of the energy flux in the wave field.

The source function, Q, of the wave system can be derived from the spatial rate of change of the energy flux:

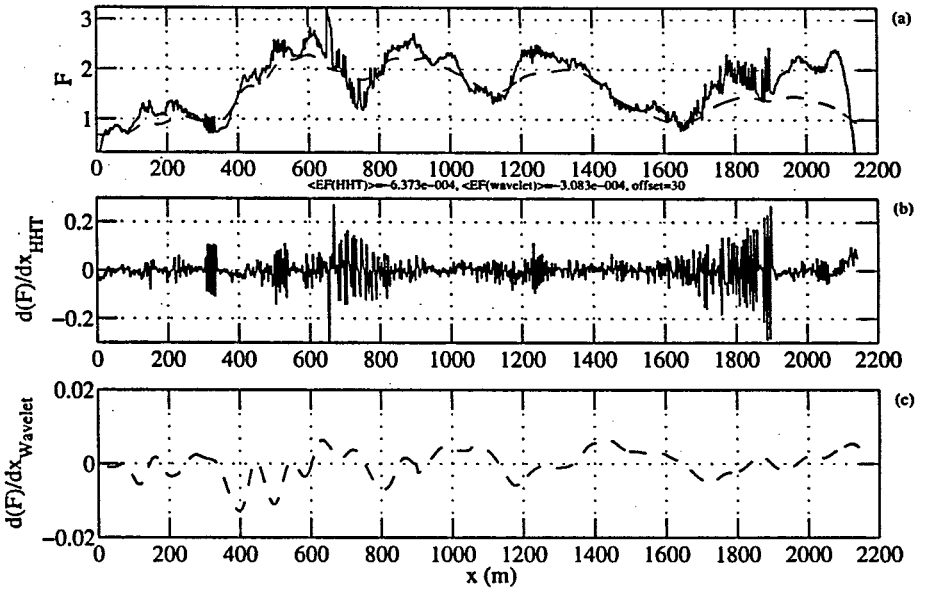

FIGURE 4.2 (*a*) Energy flux computed from the shoaling swell shown in Figure 4.1. (*b*) The source function computed from the HHT spectrum. (*b*) The source function computed from the wavelet spectrum.

$$\frac{\partial F}{\partial x} = Q \,. \tag{4.2}$$

Figure 4.2b and c shows the derived source function based on the Hilbert and wavelet spectra, respectively. The magnitude of the Hilbert source term is considerably larger than the wavelet source term (notice the difference in scale of the two ordinates). The oscillatory nature of the source function highlights the complex nature of the wave conditions in the field. The group structure can be introduced by many processes, such as wave nonlinearity, interaction among different wave components, and bathymetry-induced wave scattering. The group structure causes the source function to fluctuate between positive and negative values, as can be visualized from Equation 4.1 and Equation 4.2. Further discussion of the group structure will be presented later.

In appearance, the source functions obtained by the HHT and wavelet methods, as shown in Figure 4.2b and c, are considerably different. In reality, the apparent difference reflects the much higher temporal/spatial resolution of the HHT method. Figure 4.3 shows the results of the running average of HHT computation, with the wavelet result superimposed. With an averaging bin width of 60 elements, the running average of the HHT source function is almost identical to the wavelet source function. The spatial average (excluding the leading and trailing 90 m of the spatial coverage shown) of the source term is -2.49×10^{-4} for the wavelet processing, -5.64×10^{-4} for the HHT processing, and -4.78×10^{-4} for the running average of the HHT

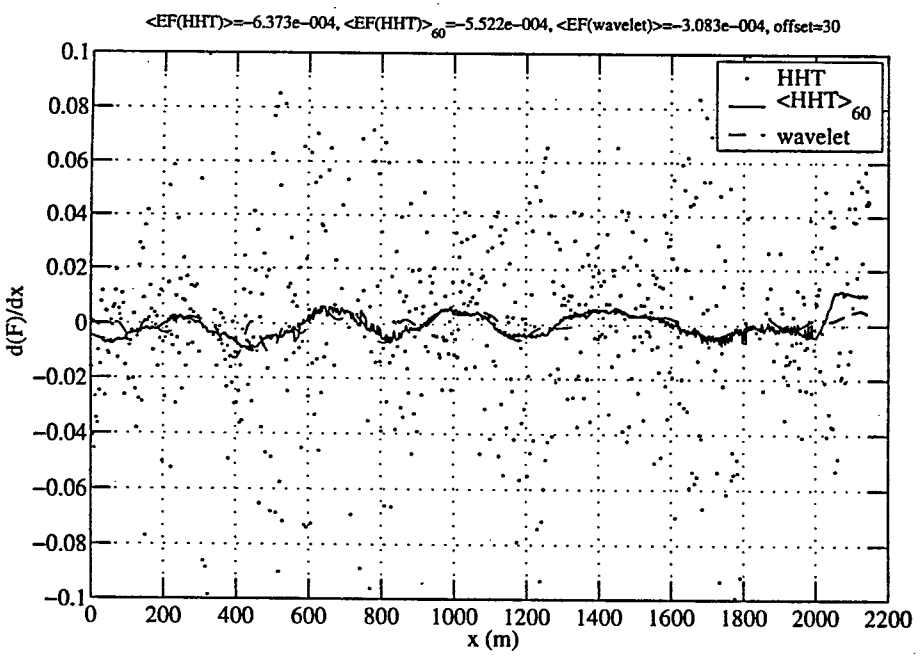

FIGURE 4.3 A comparison of the wavelet source function, the HHT source function, and the ensemble average of HHT source function with a bin width of 60 spatial elements.

processing. From this limited investigation, we conclude that the energy flux computation may be off by a factor of two using FFT based processing techniques.

As mentioned earlier, harmonic generation has created major difficulties for the analysis of wave dynamics due to the dispersive nature of water waves. For example, the phase and group velocities of each free wave component are frequency dependent, yet the harmonics (of nonlinear waves) are not dispersive. Therefore, the energy flux (the product of group velocity and spectral density) of the harmonics associated with the nonlinear waves cannot be distinguished from the energy flux of the free waves at the same frequency, and FFT based processing will always underestimate the energy flux of the wave field. The underestimation will reflect on the magnitude of parameters such as the dissipation rate or growth rate of a wave field.

4.3.2 Numerical Simulations

To investigate further the influence of processing methods and wave nonlinearity on the quantitative results of energy flux computation, numerical simulations were carried out using the refraction–diffraction (REFDEF) model [13]. The case simulated is a train of monochromatic waves (10 sec wave period and 0.25 m initial wave amplitude) propagating from offshore along a plane sloping beach. In the first scenario, the nonlinear terms are turned off, and the waveform remains sinusoidal along the full computational domain (Figure 4.4Aa). In the second scenario, the nonlinear terms are turned on, and wave asymmetry becomes obvious in the nearshore region (Figure 4.4Ba). The spatial evolution of the wave spectra for the two

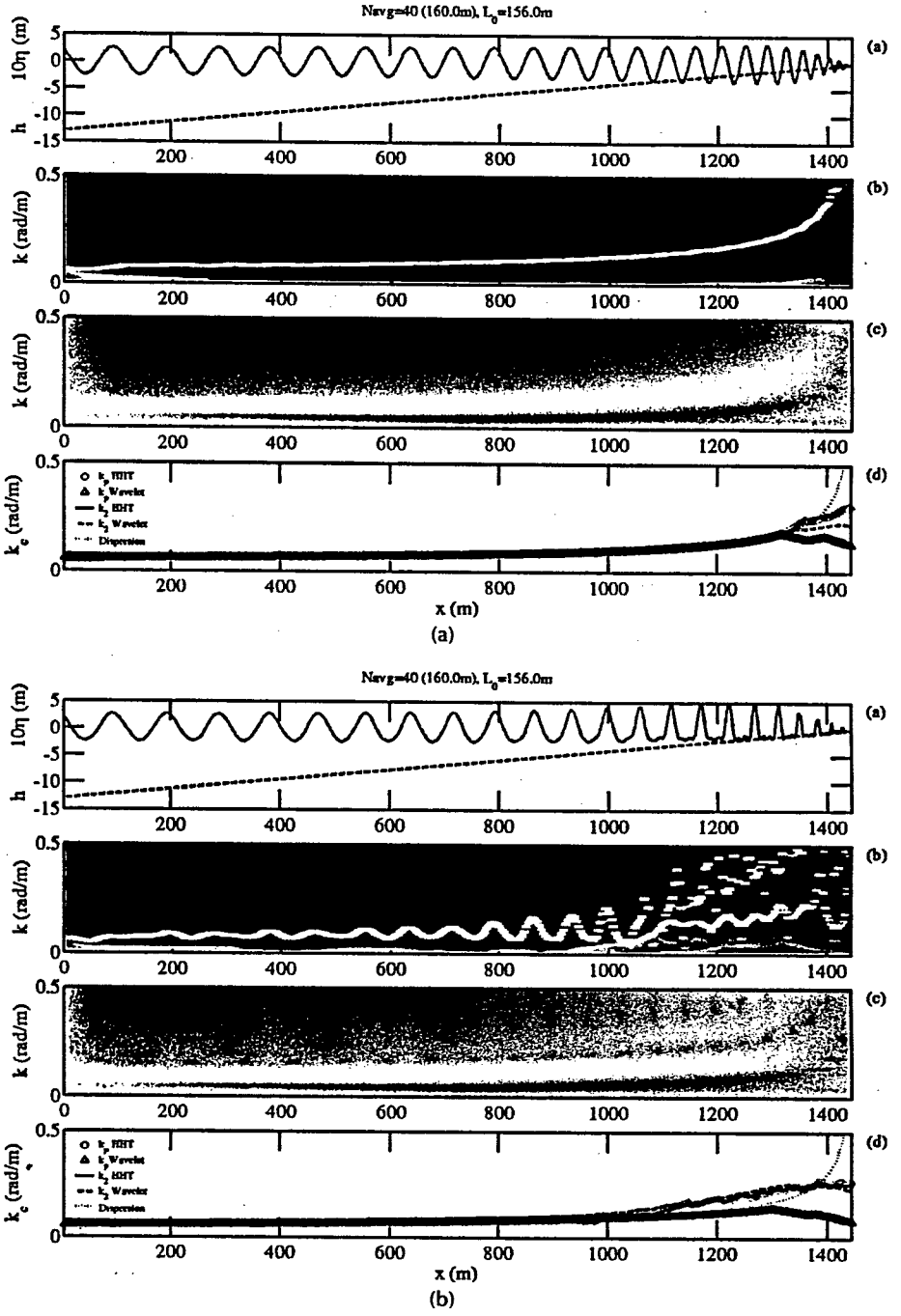

FIGURE 4.4 Numerical simulations of shoaling waves. *Left panels:* linear simulation. *Right panels:* nonlinear simulation. (*a*) Waveform and water depth, (*b*) HHT spectrum, (*c*) wavelet spectrum, and (*d*) characteristic wave numbers k_p and k_2.

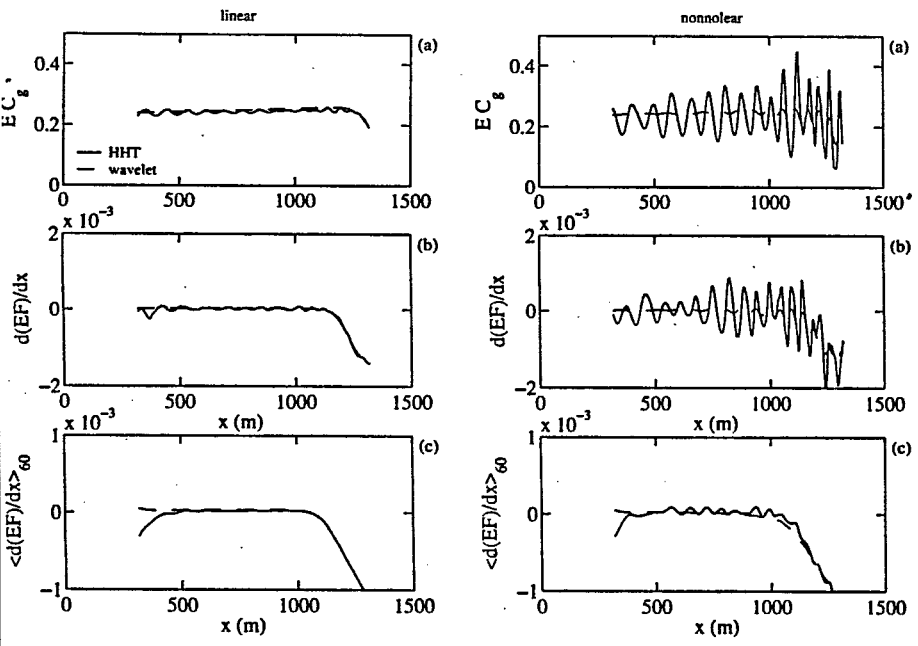

FIGURE 4.5 Same as Figure 4.4 but for the energy flux computation. (*a*) Energy flux, (*b*) gradient of energy flux, and (*c*) same as (*b*) but phase averaged. *A*: linear simulation. *B*: nonlinear simulation.

scenarios by the HHT processing method is shown in Figure 4.4b. The spectral density is concentrated in a very narrow frequency band, as expected from a monochromatic wave train. The lack of frequency modulation in the absence of nonlinearity is clear from a comparison of Figure 4.4Ab with Figure 4.4Bb. The result based on the wavelet method is shown in Figure 4.4c. The spectral energy is more spread out because of the finite window size, and the effect of nonlinearity is harmonic generation.

The characteristic wave number is typically defined as the peak wave number, k_p, or weighted wave number computed from the spectral moment, $k_n = (\int k^n S(k)dk / \int S(k)dk)^{1/n}$. With the HHT analysis, k_p and k_n are almost identical for both linear and nonlinear scenarios because the spectral energy is confined in a narrow frequency range. With the wavelet analysis, k_p and k_n are also very similar in the linear scenario, but they differ considerably in the nonlinear scenario as a result of harmonic generation. The results of phase-average k_p and k_2 for the two scenarios are shown in Figure 4.4d. Intra-wave frequency modulation as reflected by the oscillation of the characteristic wave number is clearly seen in the HHT analysis of the nonlinear simulation; it is also somewhat noticeable but much weaker in the wavelet analysis.

For the linear case, the computed energy flux and the gradient of energy flux derived from the two processing methods are very similar (Figure 4.5a,b,c). The HHT results show small intra-wave modulation due to finite amplitude of the waveform. For the nonlinear case, the intra-wave modulation is greatly amplified by the

nonlinearity of the wave system. The differentiation process in calculating the gradient of energy flux sometimes produces large spikes in the computation. The results become very sensitive to small modifications in the data processing procedure. Figure 4.5 shows an example of the processed results.

4.4 DISCUSSIONS

4.4.1 Resolution and Nonlinearity

Fourier-based spectral analysis methods have been widely used for studying random waves. One major weakness of the Fourier-based spectral analysis methods is the assumption of linear superposition of wave components. As a result, the energy of a nonlinear wave is spread into many harmonics, which are phase-coupled via the nonlinear dynamics inherent in ocean waves. In addition to the nonlinearity issue, strictly speaking Fourier spectral analysis should be used for periodic and stationary processes only. Wave propagation in the ocean is certainly neither stationary nor periodic. Using the HHT analysis, the physical interpretation of nonlinearity is frequency modulation, which is fundamentally different from the commonly accepted concept associating nonlinearity with harmonic generation. Huang et al. [1, 2] argued that harmonic generation results from the perturbation method used in solving the nonlinear equation governing the physical processes, thus the harmonics are produced by the mathematical tools used for the solution rather than being a true physical phenomenon. Through analytical examples, they demonstrated the excellent frequency and temporal resolutions of HHT for analyzing nonstationary and nonlinear signals. Here we give a few computational examples to illustrate the points discussed earlier.

Figure 4.6 presents a comparison of HHT and wavelet analysis of three different cases [3]. Case 1 is an example of an ideal time (t) or space (x) series of sinusoidal oscillations of constant amplitude; the frequency (f) or wave number (k) of the first half of the signal is twice that of the second half (Figure 4.6a). The spectra computed by the HHT and wavelet techniques are displayed in Figure 6b and c, respectively. The HHT spectrum yields very precise frequency resolution as well as high temporal resolution in identifying the sudden change of signal frequency at about the half point of the time series. In comparison, the wavelet spectrum has only a mediocre temporal resolution of the frequency change. There is also a serious leakage problem, and the spectral energy of the simple oscillations spreads over a broad frequency range (the contour interval is 3 dB in the spectral plots).

Case 2 is a single cycle sinusoidal oscillation occurring at the middle of the otherwise quiescent signal stream (Figure 4.6d). The precise temporal resolution of the HHT method is clearly demonstrated by the sharp rise and fall of the HHT spectrum coincident with the transient signal, as illustrated in Figure 4.6e. In comparison, the wavelet spectrum is much more smeared, both in the frequency and temporal resolutions (Figure 4.6f).

Case 3 is a sinusoidal function, y, with its oscillating frequencies subject to periodic modulation (Figure 4.6g)

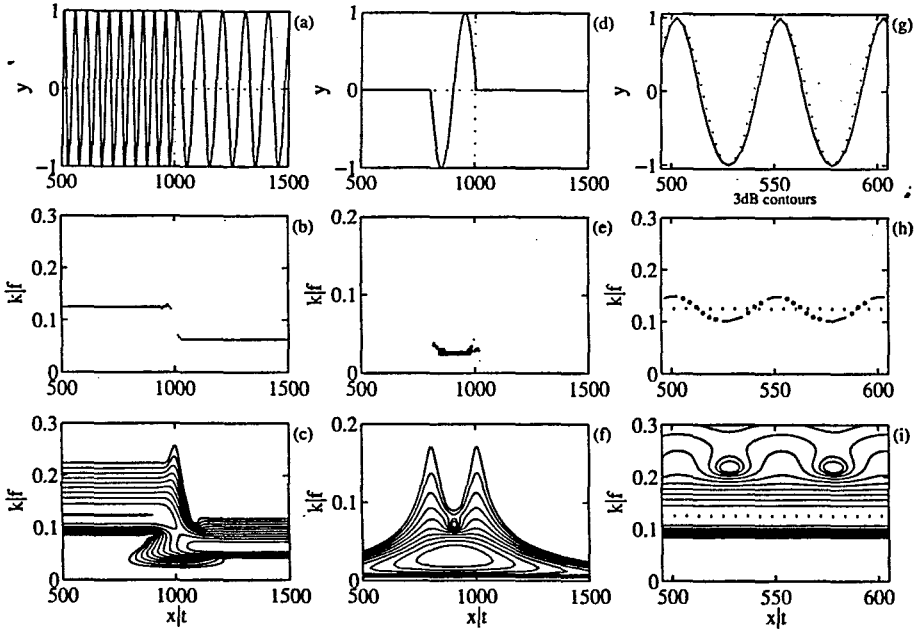

FIGURE 4.6 Examples comparing HHT (*middle row*) and wavelet (*bottom row*) analysis of nonlinear and nonstationary signals. (*a,b,c*) Time series of the harmonic motion with the oscillation period doubled in the second half, and its HHT and wavelet spectra. (*d,e,f*) Transient sinusoidal function of one cycle. (*g,h,i*) Oscillatory motion with modulated frequencies.

$$y(t) = a\ \cos\left(\omega t + \varepsilon\ \sin\ \omega t\right), \tag{4.3}$$

where a is the amplitude, ω is the angular frequency, and ε is a small perturbation parameter. This is the exact solution for the nonlinear differential equation [1]

$$\frac{d^2y}{dt^2} + \left(\omega + \varepsilon\omega\ \cos\ \omega t\right)^2 y - \left(1 - x^2\right)^{0.5} \varepsilon\omega^2\ \sin\ \omega t = 0. \tag{4.4}$$

If the perturbation method is used to solve Equation 4.2, the solution to the first order of ε is

$$y_1(t) = \cos\ \omega t - \varepsilon\ \sin^2\omega t = \cos\ \omega t - \varepsilon\left[\frac{1}{2}\left(1 - \cos\ 2\omega t\right)\right]. \tag{4.5}$$

The HHT spectrum (Figure 4.6h) correctly reveals the nature of oscillatory frequencies of the exact solution (Equation 4.3). In contrast, the wavelet spectrum (Figure 4.6i) shows a dominant component at the base frequency and periodic oscillations of the second harmonic component.

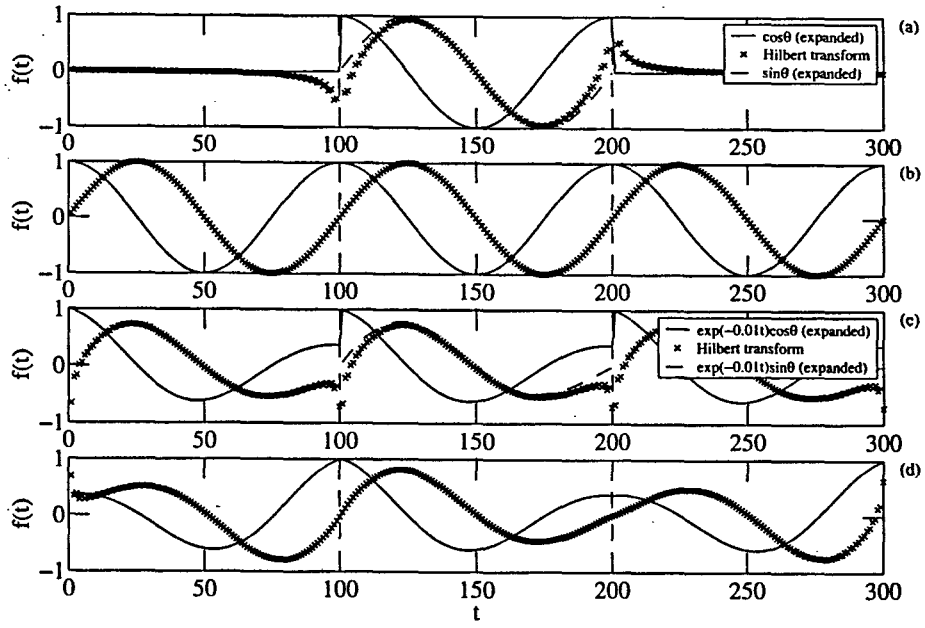

FIGURE 4.7 An example illustrating the mirror-imaging approach to alleviate edge problems.

These three examples illustrate the excellent temporal (spatial) and frequency (wave number) resolution of the HHT method for processing nonlinear and nonstationary signals. The result from Case 3 is especially interesting, as it illustrates the unique ability of the HHT technique to reveal more accurately the nature of nonlinear processes with nonstationary oscillation frequencies. Solutions obtained through the perturbation method and analysis results obtained through Fourier-based techniques represent those processes as superpositions of harmonic motions.

4.4.2 Edge Effect

One problem frequently encountered in data processing involves the treatment of the two edges of the data segment. This problem is especially serious when the data segment is short, as in many transient processes. Figure 4.7a shows an example of one sinusoidal cycle (cos t) between 100 and 300 time marks, shown by the solid curve. The Hilbert transformation of the data segment (shown by x) deviates from its exact solution, sin t, at the two edges. Padding zeros to expand the data segment does not alleviate the problem (Figure 4.7a), but repeating the signal sometimes helps, as shown in Figure 4.7b. However, if the expanded data sequence contains discontinuities (Figure 4.7c), the edge problem persists. A technique to avoid discontinuities at the two edges when expanding the data segment is to mirror image the data, as illustrated in Figure 4.7d. Our experience indicates that the edge problem can be significantly alleviated with about 30% expansion of the original data segment with the mirror-imaging method. More elaborate mirror-imaging techniques may include applying windowing (e.g., exponential decay) to the imaged segments (pri-

4.5 SUMMARY

Analyzing nonlinear and nonstationary signals remains a very challenging task. Many methods developed to deal with nonstationarity are based on the concept of Fourier decomposition; therefore, all the shortcomings associated with Fourier transformation are also inherent in those methods. The recent introduction of empirical mode decomposition [1, 2] represents a fundamentally different approach for processing nonlinear and nonstationary signals. The associated spectral analysis (HHT) provides excellent spatial (temporal) and wave number (frequency) resolution for handling nonstationarity and nonlinearity [1–3]. The HHT spectrum also results in a considerably different interpretation of nonlinearity (frequency modulation, as compared to the traditional view of harmonic generation). Applying the technique to the problems of ocean waves, we found that the spectral function derived from HHT is markedly different from those obtained by the Fourier-based techniques. The difference in the resulting spectral functions is attributed to the interpretation of nonlinearity. The Fourier techniques decompose a nonlinear signal into sinusoidal harmonics; therefore, some of the spectral energy at the base frequency is distributed to the higher frequency components. The HHT interprets nonlinearity in terms of frequency modulation, and the spectral energy remains in the neighborhood of the base frequency. This results in a considerably higher spectral energy at lower frequencies and a sharper dropoff at higher frequencies in the HHT spectrum in comparison with the Fourier-based spectra [3]. The energy flux computed by using the HHT spectrum is much higher than that obtained from the FFT or wavelet methods.

ACKNOWLEDGMENTS

This work is supported by the Office of Naval Research (Naval Research Laboratory Program Elements N61153 and N62435). This is NRL contribution BC/7330.

REFERENCES

1. Huang, N. E., Shen, Z., Long, S. R., Wu, M. C., Shih, H. H., Zheng, Q., Yuen, N. C., Tung, C. C., and Liu, H. H. (1998). The empirical mode decomposition and the Hilbert spectrum for nonlinear and nonstationary time series analysis. *Proc. R. Soc. Lond.* 454A: 903–995.
2. Huang, N. E., Shen, Z., and Long, S. R. (1999). A new view of nonlinear water waves: The Hilbert spectrum. *Annu. Rev. Fluid Mech.* 31: 417–457.
3. Hwang, P. A., Huang, N. E., and Wang, D. W. (2003). A note on analyzing nonlinear and nonstationary ocean wave data. *Appl. Ocean Res.* 25: 187–193.
4. Shen, Z., and Mei, L. (1993). Equilibrium spectra of water waves forced by intermittent wind turbulence. *J. Phys. Oceanogr.* 23(9): 2019–2026.
5. Shen, Z., Wang, W., and Mei, L. (1994). Finestructure of wind waves analyzed with wavelet transform. *J. Phys. Oceanogr.* 24(5): 1085–1094.
6. Liu, P. C. (2000). Is the wind wave frequency spectrum outdated? *Ocean Eng.* 27: 577–588.

7. Massel, S. R. (2001). Wavelet analysis for processing of ocean surface wave records. *Ocean Eng.* 28: 957–987.
8. Melville, W. K. (1983). Wave modulation and breakdown. *J. Fluid Mech.* 128: 489–506.
9. Bitner-Gregersen, E. M., and Gran S. (1983). Local properties of sea waves derived from a wave record. *Appl. Ocean Res.* 5: 210–214.
10. Hwang, P. A., Xu, D., and Wu, J. (1989). Breaking of wind-generated waves: measurements and characteristics. *J. Fluid Mech.* 202: 177–200.
11. Guillaume, D. W. (2002). A comparison of peak frequency-time plots produced with Hilbert and wavelet transforms. *Rev. Scientific Inst.* 73(1): 98–101.
12. Hwang, P. A., Walsh, E. J., Krabill, W. B., Swift, R. N., Manizade, S. S., Scott, J. F., and Earle, M. D. (1998). Airborne remote sensing applications to coastal wave research. *J. Geophys. Res.* 103(C9): 18791–18800.
13. Kaihatu, J. M., and Kirby, J. T. (1995). Nonlinear transformation of waves in finite water depth. *Phys. Fluids* 7: 1903–1914.

REPORT DOCUMENTATION PAGE

Form Approved
OMB No. 0704-0188

PLEASE DO NOT RETURN YOUR FORM TO THE ABOVE ORGANIZATION.

1. REPORT DATE *(DD-MM-YYYY)*	2. REPORT TYPE	3. DATES COVERED *(From - To)*
01-07-2005	Book Chapter	

4. TITLE AND SUBTITLE
A Comparison of the Energy Flux Computation of Shoaling Waves Using Hilbert & Wavelet Spectral Analysis Techniques

5a. CONTRACT NUMBER

5b. GRANT NUMBER

5c. PROGRAM ELEMENT NUMBER
0602435N

6. AUTHOR(S)
Hwang, Paul A., Wang, David, Kaihatu, James M.

5d. PROJECT NUMBER

5e. TASK NUMBER

5f. WORK UNIT NUMBER
73-6628-04-5

7. PERFORMING ORGANIZATION NAME(S) AND ADDRESS(ES)
Naval Research Laboratory
Oceanography Division
Stennis Space Center, MS 39529-5004

8. PERFORMING ORGANIZATION REPORT NUMBER
NRL/BC/7330--03-14

9. SPONSORING/MONITORING AGENCY NAME(S) AND ADDRESS(ES)
Office of Naval Research
800 N. Quincy St.
Arlington, VA 22217-5660

10. SPONSOR/MONITOR'S ACRONYM(S)
ONR

11. SPONSOR/MONITOR'S REPORT NUMBER(S)

12. DISTRIBUTION/AVAILABILITY STATEMENT
Approved for public release, distribution is unlimited.

13. SUPPLEMENTARY NOTES

14. ABSTRACT
The HHT analysis interprets wave nonlinearity in terms of frequency modulation instead of harmonic generation. The resulting spectrum energy concentrates in neighborhood of the fundamental frequency in comparison with the FFT or wavelet spectrum. The energy flux computation from the HHT spectrum is considerably than with the FFT or wavelet spectrum..

15. SUBJECT TERMS
HHT analysis, nonlinearity, frequency modulation; harmonic generation; FFT, wavelet spectrum

16. SECURITY CLASSIFICATION OF:			17. LIMITATION OF ABSTRACT	18. NUMBER OF PAGES	19a. NAME OF RESPONSIBLE PERSON
a. REPORT	b. ABSTRACT	c. THIS PAGE			Paul A. Hwang
Unclassified	Unclassified	Unclassified	UL	14	19b. TELEPHONE NUMBER *(Include area code)* 228-688-4708